N90-22084

A SOFT ACTUATION SYSTEM FOR SEGMENTED REFLECTOR ARTICULATION AND ISOLATION

Michael L. Agronin and Louise Jandura*

ABSTRACT

Segmented reflectors have been proposed for space-based applications such as optical communication and large-diameter telescopes. An actuation system for mirrors in a space-based segmented mirror array has been developed as part of the National Aeronautics and Space Administration-sponsored Precision Segmented Reflector program. The actuation system, called the Articulated Panel Module (APM), provides 3 degrees of freedom mirror articulation, gives isolation from structural motion, and simplifies space assembly of the mirrors to the reflector backup truss. A breadboard of the APM has been built and is described.

INTRODUCTION

The National Aeronautics and Space Administration-sponsored Precision Segmented Reflector (PSR) program is an effort to develop generic technology for space-based wide-aperture segmented reflector arrays. Mirror fabrication technology and launch vehicle cargo volume limit the size of a single mirror. Constructing an array of mirror segments in space is one means of achieving large-diameter reflectors. Applications for this technology include relatively low-precision "light buckets" for optical communication systems as well as higher-precision primary reflectors for diffraction-limited telescopes. NASA's proposed Large Deployable Reflector (LDR), a space-based 20-m infrared telescope, is an example of such an application. A concept for the LDR spacecraft is shown in Figure 1.

The current phase of the PSR program is development and demonstration of component technologies, including lightweight mirror panels, truss structures to support the mirror array, and figure control systems. The control system technologies include sensors for measuring the shape of the array, algorithms for maintaining the shape, and an actuation system for articulating the panels. The PSR articulation system design concept was first reported by Mettler, et al. [1]. This paper discusses the subsequent breadboard implementation and testing.

---

* Members of Technical Staff, Guidance and Control Section, Jet Propulsion Laboratory, California Institute of Technology, Pasadena, California

Figure 1. Concept for the Large Deployable Reflector.

TASK REQUIREMENTS

Requirements for PSR component technology are derived from several proposed NASA missions that will utilize segmented reflectors. All of the missions involve infrared diffraction-limited telescopes. LDR is the primary source of requirements for space assembly and control system capabilities. The Sub-Millimeter Explorer (SMME) and the Sub-Millimeter Imaging Line Survey (SMILS), LDR pre-cursor missions, are the sources of requirements for mirror panel, sensor, and structure development. The requirements are listed below and quantified in Table 1.

- Each mirror panel must be articulated in 3 degrees of freedom: piston (motion normal to the plane of the mirror) and tilt (rotation about the two axes in the plane of the mirror). Lateral articulation is not required, since lateral panel misalignment can be optically corrected to the first order with piston and tilt articulation. Lateral truss vibration is assumed to be much smaller in amplitude than piston and tilt vibration because of high lateral truss stiffness.

Table 1. Actuation system requirements.

Category	Requirement
Range of motion	2 mm piston, 4 mrads tilt.
Position stability	<1 μm rms in a quasi-static (no truss vibration) environment. Stability under disturbances not yet defined.
Panel size	Hexagonal, 1 m corner-to-corner.
Truss thermal strain frequency range	dc to 2 x 10^{-4} Hz, based on 90 min orbit.
Truss vibration amplitude and frequency range	Specific disturbance spectrum undetermined pending spacecraft structural analysis. For development purposes, max. amplitude < 100 μm peak-to-peak, frequency range ≥ 1 Hz.
Temperature	Materials compatible with 100K. Testing at this temperature not required during development phase.
Power dissipation at the panel	< 5 mW for three actuators. Electronics may be remotely located.
Actuator position error update rate	1 Hz max. assumed for development purposes.

- The panels must be aligned in a paraboloid whose reference frame is the focal plane of the telescope. The truss cannot be used as a reference frame for positioning panels because it is flexible and subject to thermal strains and vibrations induced by other actuators (e.g., reaction wheels, cooler pumps, solar array drives) on the spacecraft.

- Each mirror panel is parabolic. The actuation system may not distort the panel shape.

- Final assembly of the telescope will be performed by an astronaut or robot in orbit.

- Mirror temperature must be maintained as low as 100K to avoid generating infrared noise. Power dissipation must be appropriately limited.

The figure control bandwidth also puts constraints on the actuation system design. The control concept is shown in Figure 2. A figure sensing

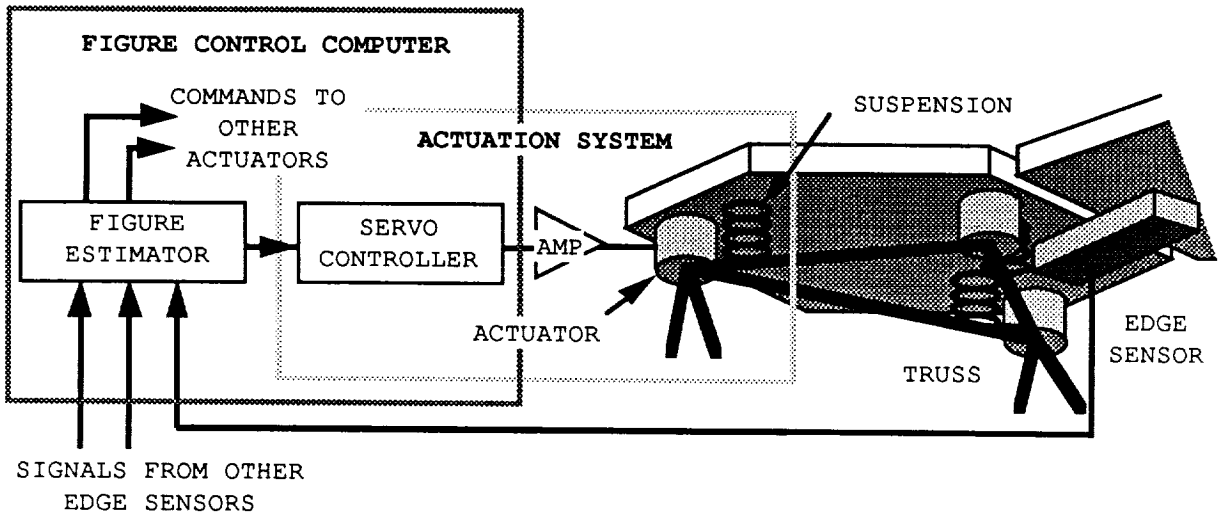

Figure 2. The figure control system.

system determines the position and orientation of each panel. Using this information, the central figure control computer calculates a position error for each actuator. The computer also processes the servo control law for each actuator. Several sensor concepts are under consideration. The edge sensor concept shown in Figure 2 uses interferometers to measure panel piston and tilt between adjacent panels, which the figure control computer transforms into an array shape. This concept is similar to the figure sensing scheme used by the Keck telescope, a 10-m segmented telescope under construction in Hawaii [2]. Whatever sensor is used, the actuator bandwidth is limited by the sensor update rate. That rate in turn depends on the number of mirrors in the array, sensor averaging time, and the computer processing speed. The update rate for the 90-panel LDR array is estimated to be as low as 0.67 Hz.

DESIGN CONCEPT: THE ARTICULATED PANEL MODULE

A design concept for the actuation scheme evolved based on the requirements described above. The biggest challenge was developing a control scheme that could isolate the panel from high-frequency truss motion with low-bandwidth feedback. The solution required complete integration of actuator, panel suspension, and control law design. Components were selected to achieve the desired system dynamic behavior.

To get around the low figure sensing update rate, we wanted to use an additional, more accessible reference frame for panel control. The moving truss cannot be used as a reference frame. However, since the panel does not have to move once the array shape is achieved, it made sense to use an inertial reference frame. Initially, we considered attaching inertial sensors to each panel, but this idea was abandoned because of the expense. Instead, we decided to use the panel's own inertia to passively isolate it from high-frequency disturbances and to use active control only for initial alignment and compensation for slow thermal truss strains. In space, the only forces acting on the panel come through the actuator and the suspension. Therefore, if the actuator and suspension are as mechanically compliant as possible, the actuation system acts as a passive low-pass filter. The design goal then is

to place the passband within the actuator's active control bandwidth. This soft actuation concept differs from the mechanically stiff systems used in other segmented reflectors such as the Keck telescope [3] or Lockheed's Advanced Structures/Controls Integrated Experiment [4], which must support mirror panels in gravity.

Actuator Selection

The electrodynamic or voice coil actuator, shown in Figure 3, was selected after an extensive actuator trade. It is ideal for a high-compliance actuation system because it produces force independent of displacement and it has zero mechanical stiffness. The electrodynamic actuator has other advantages as well. It is relatively inexpensive. Unlike a lead screw, it requires no lubrication, which eliminates the problems of contamination of optical surfaces and low viscosity at cryogenic temperatures. It also requires less complicated drive electronics than other options.

The electrodynamic actuators could have been sized to support the weight of the panel, but this would have significantly altered the design and packaging of the ground test actuators versus the flight-like versions. Instead, we decided to develop a separate gravity off-load device to support the panel's weight. With gravity off-loading (and in orbit), the actuator needs to generate only enough force to extend the suspension (0.003 N in the breadboard). At this force level, the power dissipated to a mirror by three actuators is only ~2 μW, well below the requirement.

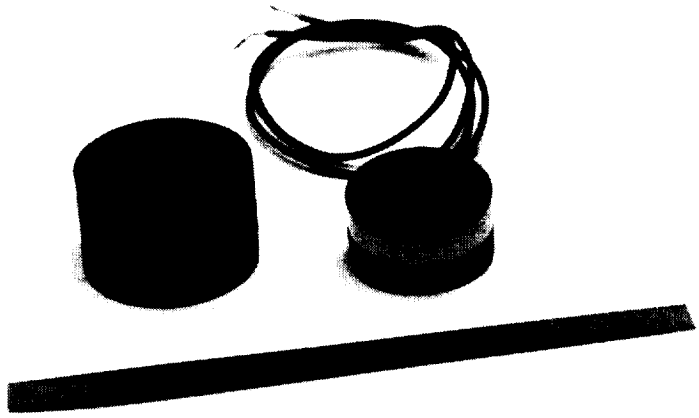

Figure 3. The electrodynamic actuator.

Suspension Design

The suspension design integrates the functions of isolation, kinematic attachment, and simplification of space assembly. The suspension assembly, including the mirror panel, is called the Articulated Panel Module (APM). An exploded view of the APM is shown in Figure 4. The panel is attached to three struts that are attached to a triangular subplane. The actuators act kinematically in parallel with the struts. The subplane is in turn attached to three truss nodes.

The struts perform two tasks. First, they stiffly restrain the panel from lateral motion, which is necessary since lateral motion is uncontrolled. However, they are extremely compliant in the controlled degrees of freedom which is consistent with the passive isolation goal. Second, they act as a kinematic mount between the panel and the subplane, allowing independent thermal growth of the panel and subplane without distorting either. The strut length and the flexure bending stiffness determine the piston and tilt suspension frequencies. The tilt stiffness can be controlled independently of the piston stiffness by selecting the radius R (shown in Figure 4) where the strut is attached to the panel. We matched the breadboard piston and tilt frequencies to within 9% of each other so the controller would have to contend with only one resonance.

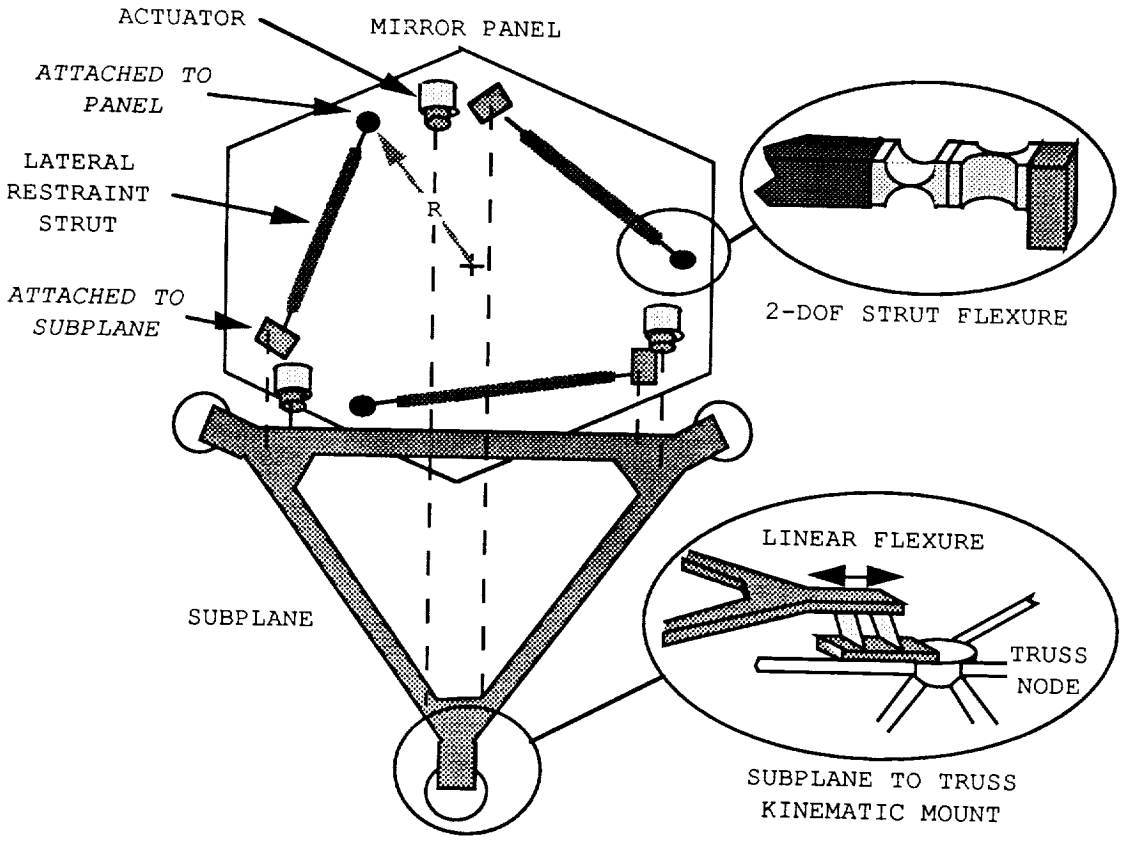

Figure 4. The articulated panel module.

The panel and actuators are attached to a subplane rather than directly to the truss, so that the suspension can be assembled, aligned, and tested before launch. The APM is a mechanically robust subassembly that can easily be attached to the truss during space assembly. The subplane has its own kinematic attachment to the truss, consisting of three linear flexures that point toward the center of the panel, as shown in Figure 4. This ensures that the subplane is not structurally redundant with the truss. The attachment is stiff to rigid body truss motion, but it allows for initial misalignments and independent thermal growth of the two structures without distortion.

Control Law Design

Taking advantage of symmetry, we used a 1-axis model of the APM for parameter selection and control law development. The model, shown in Figure 5, includes only one actuator, one strut, one-third of the panel mass, and one off-load mechanism. It is equivalent to the panel moving only in piston. We considered this model adequate for parameter selection since the piston and tilt natural frequencies are close together.

We selected a proportional-integral (P-I) control law for zero steady state error. Derivative control cannot be used because of the low (1 Hz) feedback update rate. Instead, we took advantage of the actuator's eddy current damping to provide derivative control. Eddy currents are induced in the housing of the actuator's coil piece when the actuator moves. Resistance to the eddy current is reflected back as a damping force. There is no damping from back-EMF because of a voltage feedback loop in the actuator driver.

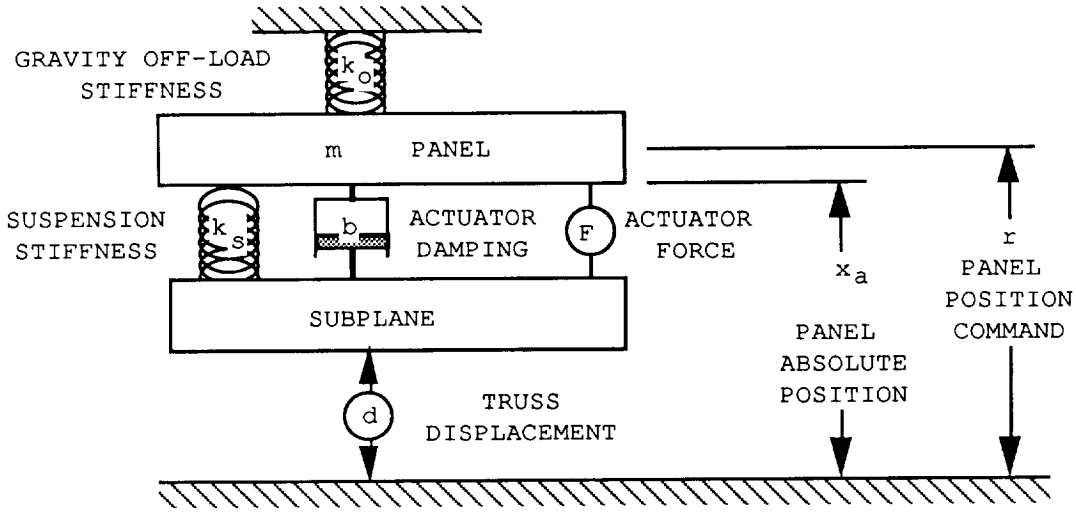

Figure 5. One-axis piston-motion model of the APM.

The closed-loop transfer function for the panel's response to a position command is:

$$\frac{x_a}{r} = \frac{\frac{p}{m}s + \frac{i}{m}}{s^3 + \frac{b}{m}s^2 + \frac{(k_o+k_s+p)}{m}s + \frac{i}{m}} \quad (1)$$

The closed-loop transfer function for the panel's response to a truss position disturbance is:

$$\frac{x_a}{d} = \frac{\frac{b}{m}s^2 + \frac{k_s}{m}s}{s^3 + \frac{b}{m}s^2 + \frac{(k_o+k_s+p)}{m}s + \frac{i}{m}} \quad (2)$$

P, the proportional gain and i, the integral gain are both normalized for sensor, actuator, and actuator driver gains in the equations above. The other model parameters are characteristics of the hardware and are defined visually in Figure 5. Parameter values, confirmed by experimentation, are listed in Table 2.

We used pole placement to select parameter values and controller gains to achieve desired dynamic performance. Pole-zero plots and their corresponding frequency responses are shown in Figures 6a and 6b. We want the damped natural frequency, labeled "C" in the figures, to be as low as possible because disturbances from the truss at frequencies above the damped natural frequency are attenuated. Truss disturbances are expected to be as low as 1 Hz. The suspension, the off-load mechanism, and the proportional gain act as springs in series which determine the damped natural frequency. The off-load mechanism should be fractionally as stiff as the suspension because we do not want its dynamics to dominate the system dynamics. We selected these parameters to put the natural frequency at ~0.2 Hz. Although it was mechanically possible to achieve a lower natural frequency, we could not accurately measure panel frequencies below 0.1 Hz.

The actuator eddy current damping controls the position of the zero labeled "D" in Figure 6b. Damping reduces the resonance peak, but it also reduces high-frequency isolation. Ideally, damping should be less than the value used in the breadboard, but the value was fixed by our actuator selection. In future implementations, the damping could be reduced by using non-conducting material in the actuator spool. The damping could also be increased, if desired, by changing the actuator driver to increase back-EMF.

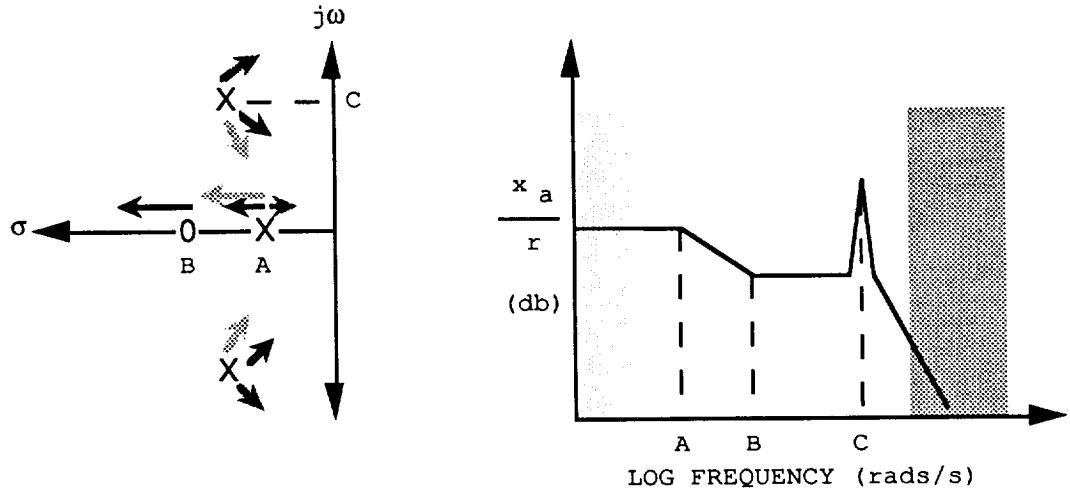

Figure 6a. Pole-Zero diagram and corresponding frequency response to position commands.

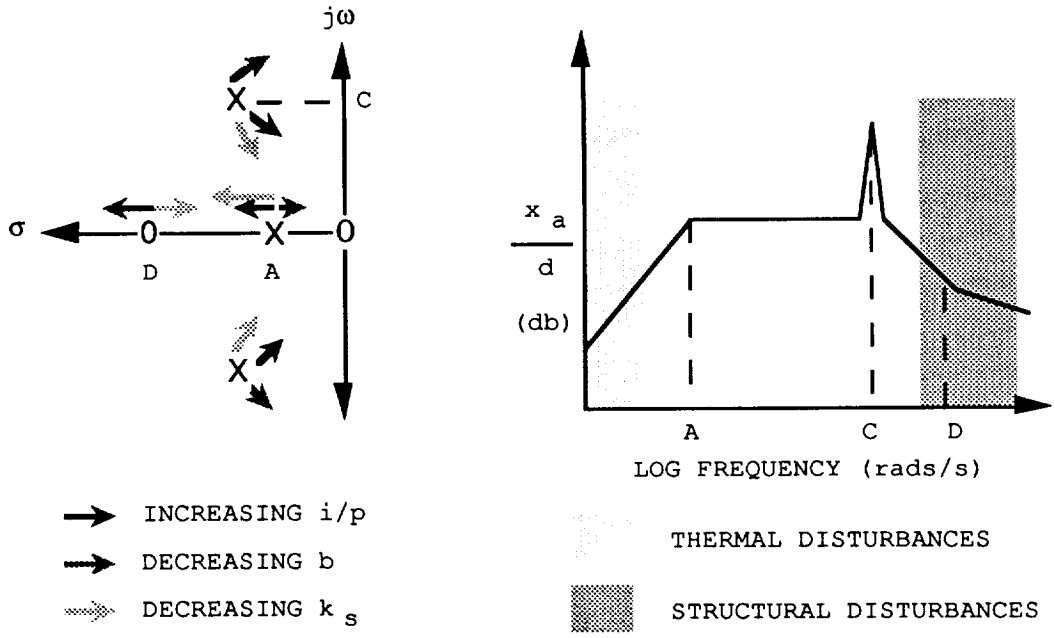

Figure 6b. Pole-Zero diagram and corresponding frequency response to truss disturbance motion.

The integral gain controls the lowest frequency pole, labeled "A" in Figures 6a and 6b, and therefore sets the command response bandwidth. The highest thermal strain frequency we have to actively compensate for is 2×10^{-4} Hz. We set the bandwidth at 0.06 Hz to achieve a reasonable step-response settling time.

Table 2. Dynamic model parameters.

Parameter	Value in 1-axis piston system (as modeled)	Value in 1-axis rotational system (as tested)
Panel mass/inertia m	2.01 kg	0.59 kg-m^2
Suspension stiffness k_s	3.68 N/m	1.24 N-m/rad
Off-load stiffness k_o	0.52 N/m	0.16 N-m/rad
Actuator eddy current damping b	3.02 N-s/m	0.91 N-m-s/rad
Proportional gain p	0.36 N/m	0.14 N-m/rad
Integral gain i	1.32 N/m-s	0.52 N-m/rad-s
System natural frequency w_n	0.24 Hz	0.26 Hz

PROOF OF CONCEPT: BREADBOARD DEVELOPMENT

We built a breadboard of the APM to test the feasibility of the design concepts as well as to explore more general control and isolation problems. In order to demonstrate feasibility, we had to emulate the APM dynamic plant, control system, and disturbance environment. We also wanted to maintain the flexibility to alter parameters and optimize the design rather than be constrained by a point design. Figures 7-9 contain photographs of the breadboard and an annotated diagram of its components.

A triangular aluminum frame, sized to approximate the mass and inertia of a mirror panel, substitutes for an actual panel. There are some differences: the triangular frame has slightly different moments of inertia in the two tilt axes, unlike the symmetrical hexagonal panel. Also, high-frequency (>20 Hz) structural resonances in the dummy panel do not coincide with actual panel modes.

The strut flexures are lengths of piano wire clamped at each end; the suspension stiffness can easily be altered by exchanging the installed wire with one of a different thickness.

The subplane is also a triangular aluminum frame. It is attached to a shaker, representing a truss node, at each corner. Closed-loop shaker control simulates truss disturbances. The shakers alone cannot support the weight of the subplane so we suspended the subplane from springs. Neither the shakers nor the springs laterally constrain the subplane, so lateral restraint struts, as in the panel suspension, tie the subplane laterally to ground.

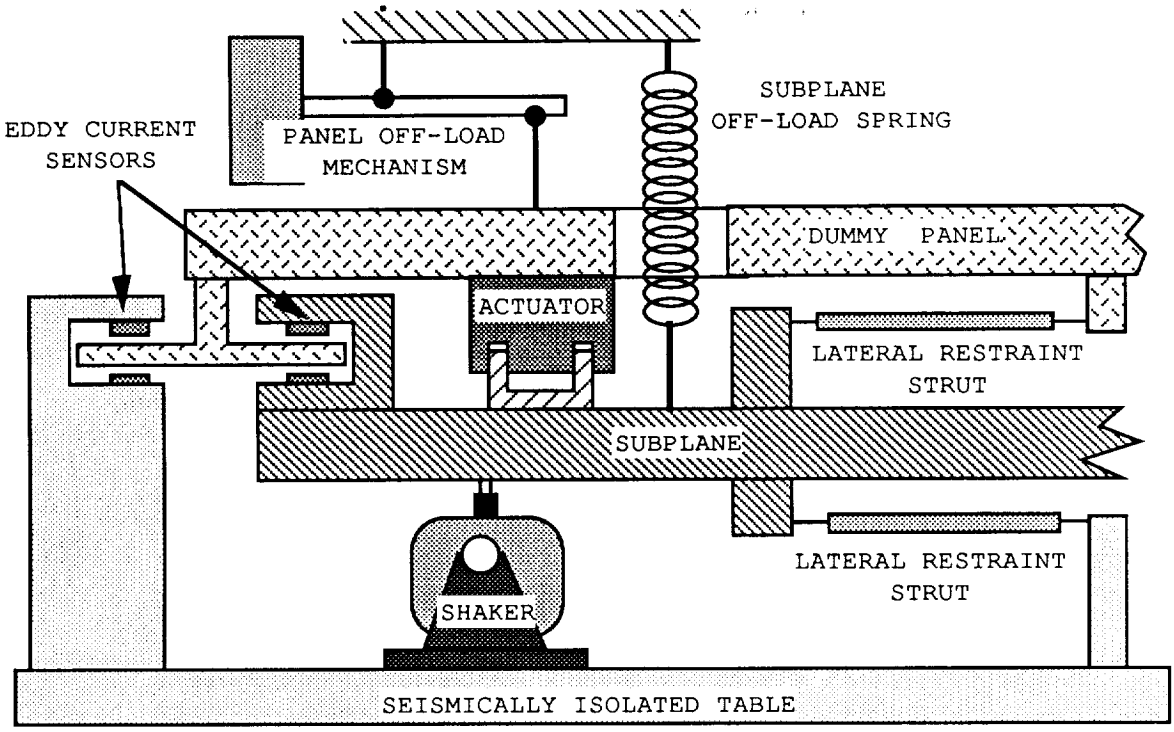

Figure 7. Schematic diagram of one corner of the APM breadboard.

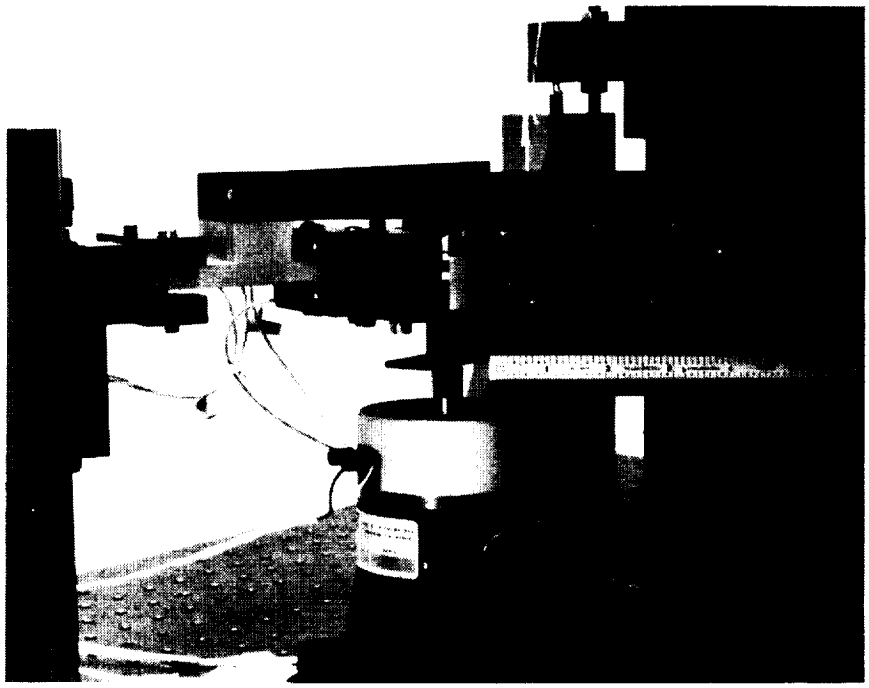

Figure 8. Photograph of one corner of the APM breadboard.

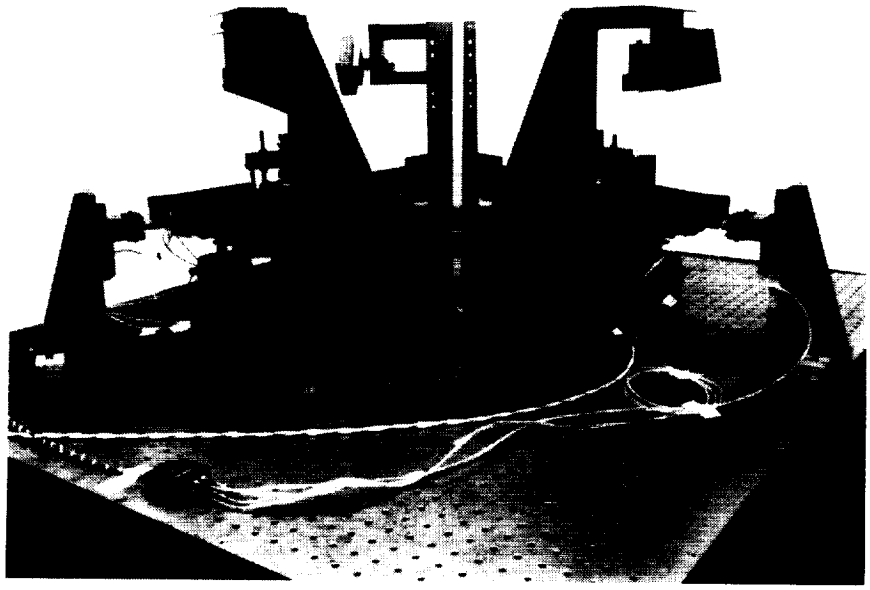

Figure 9. Photograph of the complete APM breadboard.

Eddy current sensors substitute for the figure sensor, which is still under development. The eddy current sensors measure panel-to-subplane vertical displacement and panel-to-ground vertical displacement at three points, from which piston and tilt can be determined. Subtracting the signals provides subplane-to-ground displacement for shaker control. The analog differential sensors have a 2.5-mm range and ~10-nm resolution. Sample and hold circuits added to the sensor output simulate different figure sensor update rates.

Analog circuitry emulates the servo control function of the central figure control computer. The analog boards are less expensive and easier to implement than a digital controller for the simple P-I control law.

The gravity off-load mechanism was particularly challenging because it must be fractionally as stiff as the panel suspension. We considered several options. An active off-load system was not considered because it would have been more expensive and complex than the breadboard itself. Linear springs were rejected because a spring with low enough stiffness and high enough load capacity was too long to fit in the laboratory. An overcenter mechanism, which uses a linkage to alter a linear spring's rate to near zero for small motion, was also rejected because of its mechanical complexity. A simple design using constant force coil springs was tested, but spring hysteresis prohibited its use. We finally selected a counterweight mechanism because of its mechanical simplicity and high probability of successful performance. The counterweight adds an effective mass to the panel, but that is acceptable because it is easy to account for in the system model.

The counterweight mechanism is shown in Figure 10. Three mechanisms, one at each corner, support the panel. The mechanism consists of a pivot arm with an adjustable lead weight at one end. The panel is suspended from a cord at the other end of the arm. The arm pivots on a cross flexure attached to a pylon mounted on the table. The cross flexure is designed for extremely low bending stiffness. Two lengths of cord, spaced a few inches apart, support the arm vertically. Two lengths of thin piano wire provide enough horizontal stiffness to eliminate yawing and horizontal motion.

The cross flexure adds negligible stiffness to the counterweight, but proper kinematic design is necessary to avoid pendulum stiffness. For zero pendulum stiffness, the pivot arm's center of gravity, the cross flexure pivot point, and the point from which the panel is suspended must be collinear. Stiffness is controlled by the equation:

$$k_o = \frac{-W\,h}{l^2} \tag{3}$$

where W is the weight of the panel and l and h refer to the horizontal and vertical distances, respectively, from the pivot point to the suspension point, as shown in Figure 10. The exact location of the pivot arm's center of gravity cannot be measured, especially since it moves when the lead weight is adjusted to balance the panel weight. In order to control the stiffness, h is adjustable. Notice from the equation that if h is positive (above the centerline in Figure 10), the spring constant is negative.

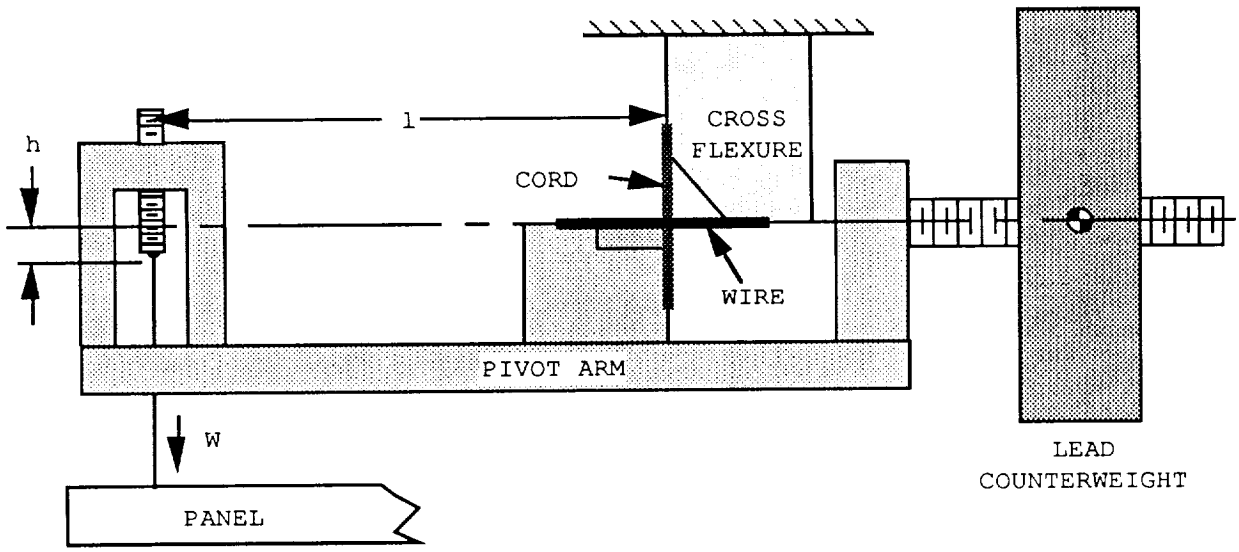

Figure 10. The counterweight off-load mechanism.

It is important to isolate the breadboard from seismic disturbances during testing; with the panel so well isolated, seismic disturbances cause the sensors to move indicating apparent panel motion. The breadboard is mounted on an optical table attached to a seismic pier. The pier is sunk in the earth through a hole in the floor of the lab and thus isolated from vibration of personnel walking down the hall, etc. Nonetheless, it was necessary to turn off the building's air handler during tests because of its seismic disturbances. We also built a "tent" over the breadboard to isolate it from air gusts; an enthusiastic gesture by one of the experimenters could drive the panel against its stops.

TEST RESULTS

The initial series of breadboard tests were intended to measure actual parameter values and validate the system model. We constrained the panel to 1 degree of freedom, as in our model, by locking the position of two of the counterweight mechanisms. The panel was free to tilt about the axis defined by the two attachment points of the locked counterweights, reducing the panel dynamics to a rotary system analogous to the linear motion system described in the model. Only one actuator and one shaker were operated for these tests. Individual parameter values measured from this rotary system are listed in Table 2. Values for the linear motion system were derived from the rotary system measurements.

The panel frequency response to position commands was measured by driving the actuator with white noise and recording the response with a spectrum analyzer. In Figure 11, the actual response is compared with the transfer function from Equation 1. Similarly, isolation from truss motion was measured by driving the shaker with white noise while the panel was commanded to hold a constant position. In Figure 12, experimental result is compared to that predicted by the transfer function from Equation 2. This figure shows that the optical table resonance as well as panel structural resonances were excited, results not considered in our model. Although the breadboard does not correspond structurally to a flight-like APM, the APM may share this problem if large-amplitude truss disturbances occur at its structural resonance frequencies.

Position stability and step response under no disturbance is shown in Figures 13 and 14. The system achieved 0.07 μm rms position stability over 15 s, well below the 1 μm rms stability requirement. Settling time to a step command is approximately 20 s.

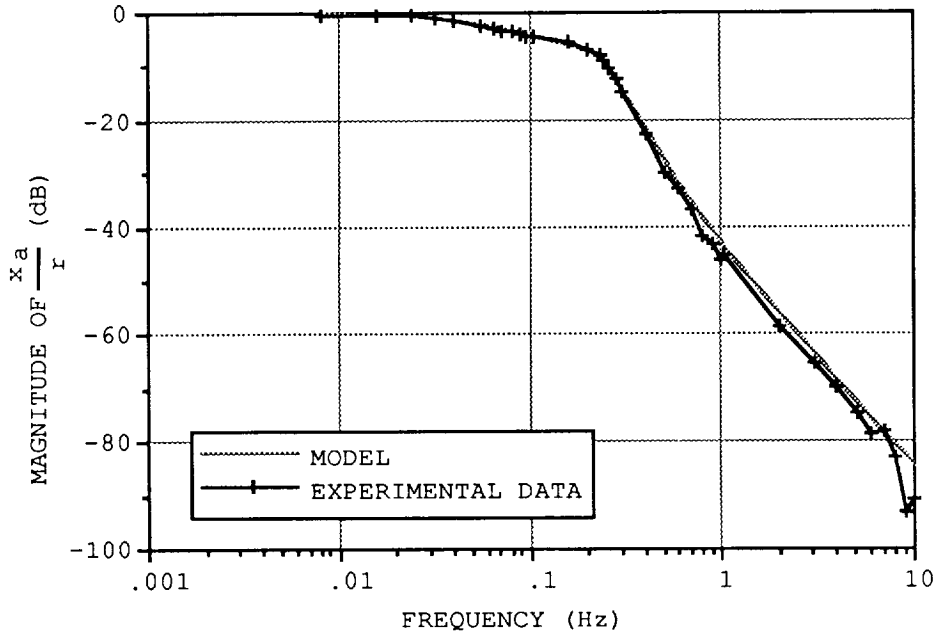

Figure 11. Predicted and experimental frequency response to position commands.

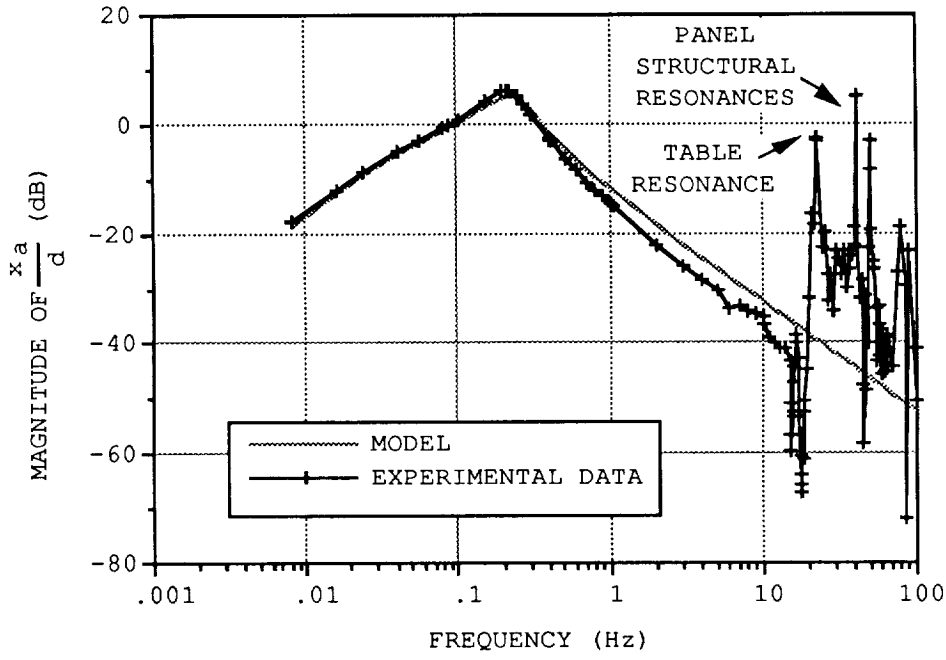

Figure 12. Predicted and experimental frequency response to truss disturbance motion.

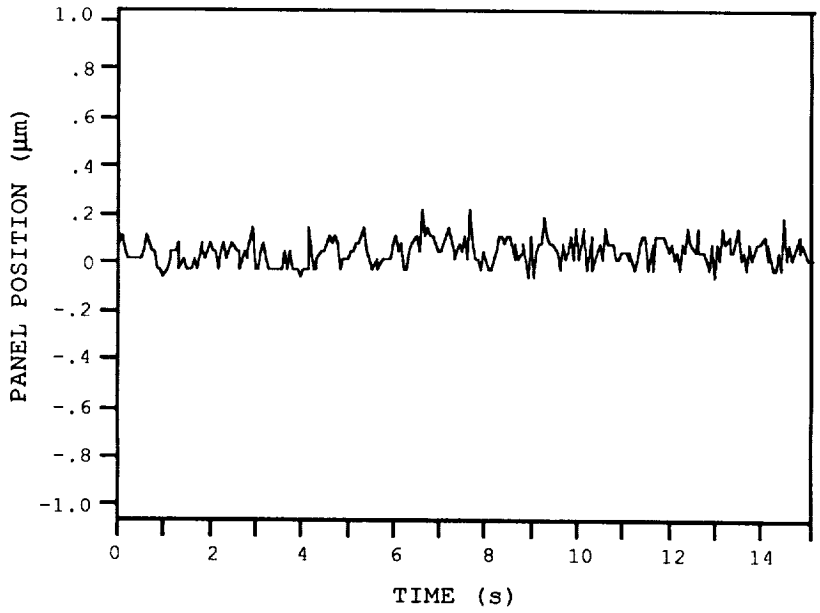

Figure 13. Panel position stability.

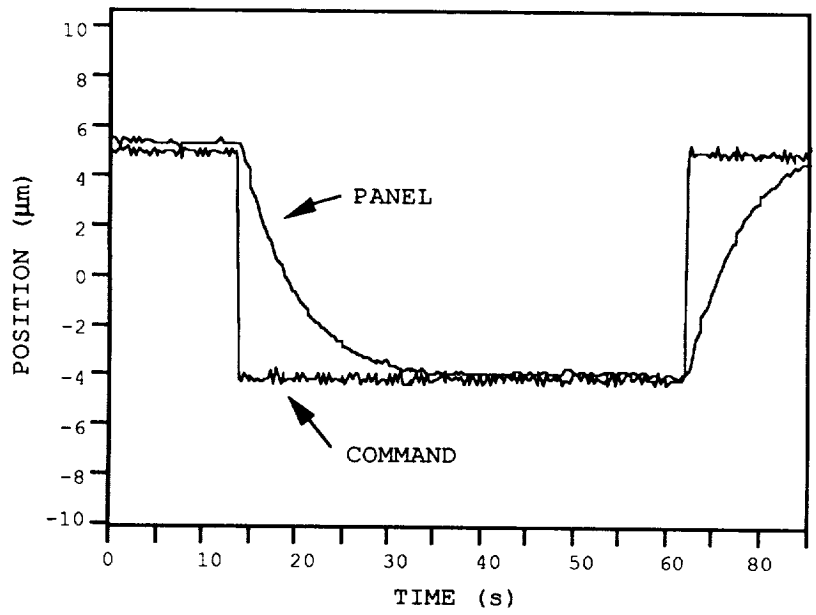

Figure 14. Panel step response to a position command.

FUTURE WORK

The next phase of breadboard testing will be to operate all three axes and compare performance to a three-axis model. After modeling the disturbance environment of a spacecraft in the focus missions, disturbance rejection requirements will be better defined, and design of an engineering model of an APM will proceed. Eventually, the PSR program hopes to demonstrate the complete figure control system with an array of APMs.

CONCLUSIONS

Thus far, all of the APM performance requirements have been met or exceeded. The APM shows great promise as a means of controlling and isolating mirrors or other optical components in limited degrees of freedom, with considerably less expense and complexity than a magnetic suspension. The authors hope that the design concepts used in the APM can be extended to other precision articulation and isolation applications.

REFERENCES

[1] Mettler, E., et al.: "Precision Segmented Reflector Figure Control System Architecture," presented at the S.P.I.E. Conference on Active Telescope Systems, Orlando, FL, March 1989.

[2] Gabor, G.: "Position Sensors and Actuators For Figure Control Of A Segmented Mirror Telescope," S.P.I.E., Vol. 172, p. 39, Instrumentation in Astronomy III, 1979.

[3] Gabor, G.: "Actuators For A Segmented Mirror Control System," S.P.I.E., Vol. 444, p. 287, Advanced Technology Optical Telescopes II, 1983.

[4] Lorell, K. R., et al.: "Development Of A Precision, Wide-Dynamic-Range Actuator For Use In Active Optical Systems," Proceedings of the 23rd Aerospace Mechanisms Symposium, p. 139, 1989.

ACKNOWLEDGMENTS

The PSR control system architecture was conceived by Edward Mettler, Daniel Eldred, Hugh C. Briggs, Taras Kiceniuk, and Michael Agronin. The authors wish to acknowledge the substantial contributions to this research by other members of the PSR Figure Control Team: Russ Allen, Dhemitrious Boussalis, and George Sevaston.

This work was performed at the Jet Propulsion Laboratory, California Institute of Technology, under contract for the National Aeronautics and Space Administration.